

Variability in The Vertical Conductivity of Granular Sea Ice

C. Sampson¹, Y. Chung⁴, D. Lubbers³, and K. M. Golden²

¹ University of North Carolina at Chapel Hill, Department of
Mathematics

²University of Utah, Department of Mathematics

³University of Utah, Department of Electrical Engineering

⁴University of North Carolina at Greensboro, Department of
Mathematics and Statistics

Abstract

The crystallographic structure of sea ice influences many of the key physical processes in the polar regions all of which play a major role in the Earth's climate system. There has been much recent interest in using electrical methods to remotely monitor temporal variations in the ice pack to aid in improving models of these key processes. Important to these models is the crystallographic structure of the ice which is difficult to determine electrically. In September-October 2012, in conjunction with crystallographic analyses, we made direct measurements of the vertical component of the bulk conductivity of first year Antarctic sea ice as participants in the Sea Ice Physics and Ecosystem Experiment II (SIPEX II). We found higher levels of local variability in the vertical DC conductivity of granular sea ice than that of columnar sea ice. This variability is related to the differences in the way vertical connections grow in the two ice types. This work suggests that the vertical component of conductivity may be used as an aid in electrically determining the crystallographic structure of sea ice.

1 Introduction

The polar sea ice packs play a critical role in regulating the Earth's climate system and serve as sensitive indicators of climate change. In particular they play a major role in regulating gas exchange in the polar regions and are an important factor in the Earth's over all albedo. These important large scale processes depend on small scale processes within the ice. For example, fluid flow through the porous sea ice is a major controlling component in the evolution of melt ponds which in turn affects the ice pack albedo [9], brine drainage and the

evolution of salinity profiles [39, 8], snow ice formation, where sea water floods the ice surface and then freezes [25], ocean ice-atmosphere CO_2 exchanges [31], convection enhanced thermal transport [23, 38], and biomass build up fueled by nutrient fluxes [34, 10, 22, 6]. Important properties such as fluid flow exhibit critical behavior which depends on the crystallographic structure of the ice. For example in columnar ice it has been shown that the ice is effectively impermeable below brine volume fractions of 5% [14] while granular ice is impermeable for brine volume fractions below about 10% [15]. When using small scale models to understand these processes the importance of knowing the crystallographic structure becomes paramount. Recently investigations into using DC resistivity to remotely monitor the growth and evolution of sea ice throughout a season have shown promising results [21, 18, 30, 13] however most of the studies focus on columnar ice and fail to resolve ice type with the exception of the detection of increased horizontal conductivity at the skeletal/platelet layer at bottom of fast ice [20]. While columnar ice is the most prevalent ice type in the Arctic, although the upper 10 cm of Arctic ice is typically granular, the situation in the Antarctic is the drastically different. Nearly 40% of the Antarctic ice pack is made up of granular ice, of which, nearly a quarter is fine grained granular snow ice [25, 19, 40, 7], with even higher fractions in some regions[26]. Given the importance of ice type in relation to many important physical processes in the ice, it is thusly important to include a method to detect ice type in any remote sensing scheme.

We view sea ice as a two phase polycrystalline composite material made up of ice and brine, with the brine phase conducting and the ice phase insulating. In this way, the conductivity of the ice depends on the connectivity of the brine phase throughout the ice column and exhibits critical behavior similar to fluid flow at the 5% threshold[13]. In studies of polycrystalline composites the crystal orientation plays a major role in the properties of the given material such as electrical permittivity and conductivity [27, 5, 16]. Columnar sea ice crystals are typically oriented together with a horizontal c-axis while granular sea ice crystals are randomly oriented [29, 2, 8]. The crystal morphology has an impact on the way in which vertical connections in the pore space of sea ice form and connect. This leads to a higher variability of the electrical properties in the vertical direction for granular sea ice on small local scales. It is this variability that can be exploited to electrically detect ice type.

During September through November of 2012, we made measurements of the vertical conductivity of first year columnar and granular sea ice off the east coast of Antarctica as participants in the Australian Sea Ice Physics and Ecosystem Experiment (SIPEXII) aboard the ice breaker Aurora Australis. In this paper we compare that data to some established results as well as present an analysis of local scale variability of the electrical properties of granular ice which differ from that of first year columnar ice.

2 Methods and Measurement

In order to directly measure the vertical conductivity of the ice we employed a Wenner electrode array along 10 cm sections of our ice cores, as illustrated in Fig 1. This method is similar to that used in [13]. To make the measurement we used a AEMC DC resistivity meter. To facilitate the measurement, full length ice cores were extracted and holes were first drilled into the cores at 10 cm intervals and temperature probes inserted along the core. Next, slightly larger diameter holes were drilled into the previous temperature probe holes with tight fitting nails inserted and used as electrodes for the Wenner array. The nails were slightly larger than the holes to ensure a good electrical connection with the ice. With a 10 centimeter spacing between electrodes, current was injected by the outer probes and the potential difference measured at the inner two. This gave the resistance for the 10 cm section of the ice between the innermost probes. The cores were then bagged and rushed into a -22°C crystallography lab on board the Aurora for later analysis. In the lab the cores were cut into 10cm sections at the measurement holes and vertical thin sections cut from the center of the sections were extracted and placed between two cross-polarizing films showing the crystal structures of the corresponding to the resistance measurements. The outer halves of the sections were bagged and melted for bulk salinity measurements. The crystallography lab was cold enough to completely freeze the cores to minimize brine leakage. The temperature(T) $^{\circ}\text{C}$ and bulk salinity (S) PSU can then be used to calculate the brine volume fraction ϕ corresponding to the resistance measurement using the Frankenstein-Garner relation shown in eq 1.

$$\phi = \frac{S}{1000} \left(\frac{49.185}{|T|} + 0.532 \right) \quad (1)$$

The vertical conductivity of a 10 cm section can be found using the measured resistance R . The vertical resistivity ρ_v and corresponding conductivity σ_v are obtained via $\rho_v = AR/L$, $\sigma_v = 1/\rho_v$ where A is the cross sectional area and L the length.

3 Theory

3.1 Conductivity in Columnar and Granular ice

As sea water begins to freeze the first ice crystals to form create a slush referred to as frazil ice. As this slush freezes granular ice forms which has crystals with random c-axis orientations that trap brine in between them. As further growth progresses, crystals which have their c-axes aligned in the horizontal plane grow downward leading to the formation of vertical columns of ice dubbed, columnar ice. An example of this ice can be seen in Fig 1a. In this type of ice brine inclusions and vertical tubes form between the subgrains of the ice aligned with the growth directions of the crystals [8]. At low temperatures

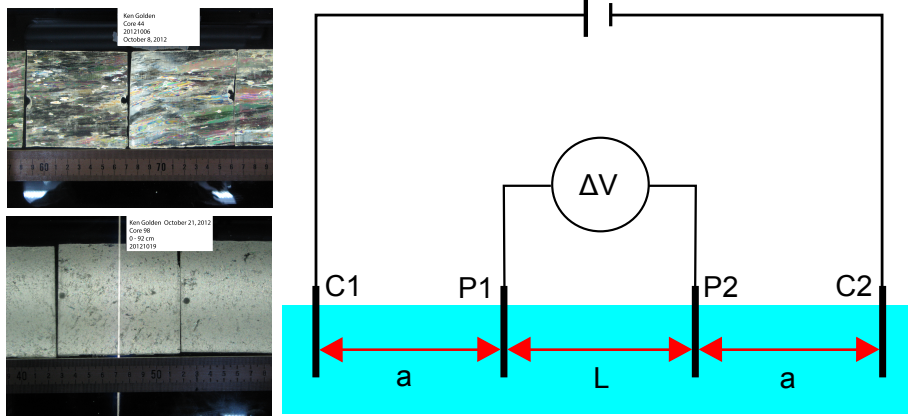


Figure 1: Left: Images of columnar and granular crystallographic samples corresponding to the 10cm measured sections. Resistivity measurements were made between the holes in the thin sections. Right: A schematic of the Wenner array setup used to measure the vertical component of the ice core. The measurement corresponds to the length L between P_1 and P_2 .

the brine inclusions are smaller and isolated from each other. As the sea ice warms they begin to connect up forming long vertical pathways within the ice [8, 14]. This vertical alignment leads to anisotropy in the conductivities of the ice as current flows preferentially along the elongated brine inclusions yielding an increased vertical conductivity. In addition, sea ice is typically transversely isotropic [30, 32] yielding the same conductivities in all horizontal directions. The electrical anisotropy in transversely isotropic materials like sea ice can be quantified using the factor of anisotropy defined as $f = \sqrt{\sigma_h/\sigma_v}$ [24, 30]. One can quantify the level of crystallographic anisotropy using the crystal anisotropy factor. This is defined as defined as $A = \Sigma C_v / \Sigma C_h$, where C_v and C_h are the size of the vertical and horizontal projections of each individual c-axis measurement from a thin section. For both parameters a value of 1 indicates isotropy while $A = 0$ indicates that all c -axes lie in the horizontal plane. Examples of values of A are $A = 0.23$ and 0.14 for columnar ice and $A = 0.67$ for platelet ice [20]. Typical values of f range from 0.2 to 0.7 with the higher values possibly indicating granular ice[30, 32]

In contrast to columnar ice, granular frazil and granular snow ice are comprised of crystals with isotropically distributed c-axes which trap the conductive brine between them. Given its structure one might expect granular ice to have an isotropic bulk conductivity, however this is not the case. The conductivity in the vertical direction remains larger and does not differ much from that of columnar ice. This may suggest that anisotropic secondary pores (such as brine tubes and channels which form as the ice warms and gravity pulls the

brine down) control the resistivity structure rather than the isotropic primary pore space [21]. This is consistent with our findings as well as we see no clear difference in the overall vertical conductivities of our granular and columnar measurements as a whole. However, the horizontal conductivity of granular ice is typically higher. This has been observed in [20] using cross-borehole tomography to measure the horizontal and vertical conductivities of first year Antarctic sea ice. They found increased horizontal conductivities near the upper granular layer of the ice as well as near the bottom platelet layers. This was attributed to a larger number of horizontal connections that result from the more random crystal structure of the ice [20]. They were also able to show that as crystallographic anisotropy A increased the factor of electrical anisotropy f increased as well. This implies that as the crystal structure of the ice becomes more isotropic, the bulk conductivity does as well.

3.2 Thermal Evolution of Columnar and Granular ice

Given the electrical anisotropy of sea ice and the apparent control of its resistivity structure by the connectivity of the brine inclusions, it is important to understand how these structures evolve with increases in temperature and porosity. In particular, we are interested in the how vertical connectivity of the pore space changes as it is the controlling factor in the vertical conductivity of sea ice.

The evolution of connectivity in columnar ice has received more attention than that of granular ice [8, 14] however it is clear in these studies that as the temperature of columnar sea ice increases, and thus porosity, the pore space connections that form are oriented primarily in the vertical direction and reside between the vertically aligned columnar ice crystals. It is only at high brine volume fractions that more complicated geometry is observed. In a NMR study [3] of the thermal evolution of pore space connectivity of samples of winter columnar and granular sea ice taken near Barrow Alaska, it was observed that the connections which formed in the granular samples, as temperature was increased, had a more complex morphology with a combination of horizontal and vertical connections. Those of the columnar sea ice were primarily vertical and constrained within the lamellar plane of the columnar ice crystals. This difference in the evolution of connectivity has implications for the behavior of the vertical conductivity of a localized region of granular or columnar sea ice. We see evidence of this in our thin sections as well, illustrated in figure 2. The two granular sections in the figure are from core 99 and have brine volume fractions of $\phi = 0.834$ and $\phi = 0.836$ but differ with vertical formation factors, defined as the ratio of the conductivity of the ice to that of the brine, of $F_v = 0.02$ and $F_v = 0.011$ respectively with the higher conductivity corresponding to the sample with the elongated vertical connection. In [14] it was observed that the fractional connectivity, defined as the proportion of inclusions at the upper surface which are also connected to the lower surface, for a cylindrical sample of lab grown columnar sea ice increased linearly with increasing porosity for brine volume fractions above $\phi_c = 5\%$. While no similar data for granular ice

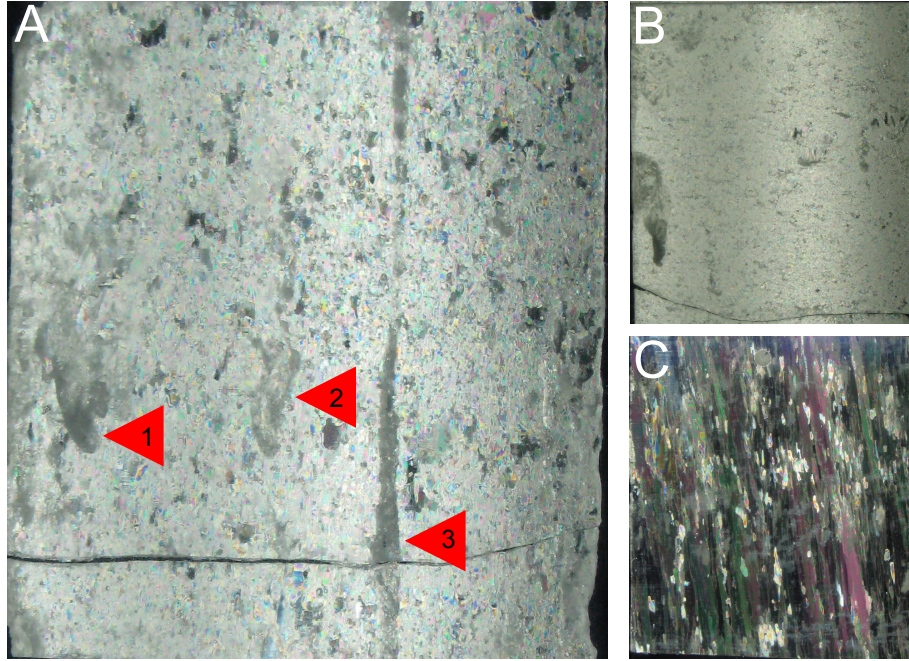


Figure 2: A: 10 cm section of granular ice from core 99. Arrows 1 and 2 indicate pore spaces with complex morphology while arrow 3 shows a vertical connection which acts as the primary control of the resistivity structure. B: 10 cm section of granular ice from core 99 with a similar brine volume fraction to the section shown in A, but with little to no vertical connectivity. C: 10 cm section of columnar ice from Core 44 showing the vertical alignment of the pore spaces between columnar crystals.

was found, we would expect different behavior. Due to the random distribution of the c-axes of the ice crystals in granular ice, there is less to constrain the direction of the pore space expansion with an increase temperature. This would imply a variety of levels of vertical connectivity for a given brine volume fraction in granular ice and thusly a wider variation in values of vertical conductivity.

3.3 Percolation Theory and Critical Behavior

Percolation theory for both lattice and continuum models applies to materials where the connectedness of one phase dominates the effective behavior of the material as a whole. In sea ice it is the connectedness of the brine phase which dominates the effective electrical properties of the ice as a whole [13].

Consider the infinite square ($d = 2$) or cubic ($d = 3$) network of bonds joining nearest neighbor sites on the integer lattice \mathbb{Z}^d . The bonds are assigned

conductivities of $\sigma_0 > 0$ (open) or 0 (closed) with probabilities p and $1 - p$ respectively. There is a critical probability p_c called the *percolation threshold* where an infinite, connected set of open bonds first appears. In $d = 2$ $p_c = 1/2$ and in $d = 3$ $p_c \approx 1/4$. Let $\sigma(p)$ be the conductivity of this random network of bonds in the vertical direction. For $p < p_c$, $\sigma(p) = 0$. For $p > p_c$, near the threshold $\sigma(p)$ exhibits power law behavior,

$$\sigma(p) \sim \sigma_0(p - p_c)^t \quad \text{as} \quad p \rightarrow p_c^+, \quad (2)$$

where t is the conductivity critical exponent. In $d = 3$, it is believed that $t \approx 2$ [36, 37] and there is a rigorous bound [11] that $t \leq 2$.

In [13] it was observed that the vertical conductivity of columnar sea ice exhibits critical behavior at a critical brine volume fraction $\phi_c \approx 5\%$. This corresponds to the volume fraction in the *rule of fives* [12] where the brine channels first begin to connect on large scales. Below this percolation threshold the vertical conductivity, while not zero, shows slow growth while after this threshold, when the brine phase begins to connect on a large scale, the conductivity increases very rapidly and can be modeled with percolation theory according to the equation

$$F_v(\phi) = F_0(\phi - 0.05)^2 = 9(\phi - 0.05)^2, \quad (3)$$

again where $F_v(\phi) = \frac{\sigma_v}{\sigma_b}$ is the vertical formation factor defined as the ratio of the vertical conductivity σ_v and the conductivity of the brine σ_b . The conductivity of the brine can be calculated from the temperature T via [33]

$$\sigma_b = -T \exp(0.5193 + .08755T) \Omega^{-1} m^{-1}, \quad T \geq -22.9^\circ C. \quad (4)$$

The scaling factor F_0 is estimated in [13] to fall in a range of $6 \leq F_0 \leq 24$ for columnar ice via critical path analysis. The factor $F_0 = 9$ comes from a statistical best fit of vertical conductivity data from the SIPEX I cruise in 2007.

3.4 Archie's Law

Archie's law [1] is an empirical equation relating the bulk conductivity σ^* of a porous medium to its porosity and the conductivity σ_f of the fluid occupying the pore space,

$$\sigma^* = a\sigma_f\phi^m. \quad (5)$$

In this relation ϕ is the relative volume fraction of the fluid volume, or porosity, and a is a scaling factor often taken to be 1, which yeilds the correct limiting behavior as $\phi \rightarrow 1$. The exponent m depends on the geometry of the solid phase of the porous medium, such as the shape of the grains in porous rock or sand.

While percolation theory describes conductivities well for $\phi > 5\%$, Archie's Law is useful as it can describe the conductivity for systems with connectivity all the way down to $\phi = 0$. For our purpose we take $\sigma^* = \sigma_v$, $\sigma_w = \sigma_b$ and ϕ to be the brine volume fraction of the ice. We can then look at the vertical formation factor

$$F_v = \frac{\sigma_v}{\sigma_b} = a\phi^m, \quad (6)$$

where σ_b depends on temperature via eq 4. Archie's law has been employed to model the conductivity of ice successfully by many others [35, 30, 21, 4]. These previous results find a relatively wide range of exponents $m = 1.5 - 2.88$ for the conductivity of the ice and were measured indirectly. In [30] it was found that $m = 1.75$ was appropriate for the vertical component of the conductivity σ_v . When analyzing our data set as a whole we find good agreement with the exponent $m = 1.75$ using statistical best fits and enforcing a condition of $a = 1$. However when a is allowed to be determined by the data we obtain $F_v = .36\phi^{1.38}$, the values for a and m remain close for both the granular and columnar sets when analyzed separately.

One of the underlying assumptions in Archie's Law is that porosity and connectivity vary continuously together. If we wish to apply Archie's Law to the vertical conductivity of sea ice we must assume that small changes in porosity will give rise to small changes in vertical connectivity. This is certainly true in columnar ice, as evidenced by the TDA analysis, for $\phi > 0.05$, due to the preferential alignment of the crystals and linear growth of fractional connectivity mentioned above. However, in granular ice and in particular fine grained granular ice, where the crystal c-axes are isotropically distributed, small changes in porosity may lead to increases in horizontal connectivity rather than simply vertical connectivity. Depending on how the crystals are distributed one would expect a larger variation in the vertical formation factor of granular ice at a given brine volume fraction. Indeed, when considering the vertical fluid permeability of granular ice, it is shown in [15] that the ice is effectively impermeable for brine volume fraction below $\phi_c \approx 10\%$. In contrast, in [14] it is shown that columnar ice becomes vertically permeable at a lower critical volume fraction of $\phi_c \approx 5\%$. This illustrates that vertical connections grow more slowly in granular ice than columnar as brine volume increases. That is to say, there is only a large enough number of vertical connections for fluid flow at highly connected states. For these reasons we expect that granular ice will show more variation in F_v with brine volume fraction on the local scale than columnar ice. We also expect to see less of a power law behavior at the local scale due to the increased variability.

4 Results and Discussion

4.1 Comparison to Established Results

In this section we will simply compare our data to established results. In relation to Archie's Law for the vertical formation factor $F_v = \phi^m$, we performed statistical best fits on our data sets separated by ice type as well as the combined data set. We performed fits forcing the scaling parameter $a = 1$ and obtained $m = 1.76$ for our granular ice and $m = 1.71$ for columnar ice. When combining the data sets we obtain $m = 1.75$. These results are in close agreement with the value of $m = 1.75$ measured for the vertical conductivity and assumed by others [17, 28, 30].

When considering percolation theory it is useful to instead look at the vertical resistivity factor, $R_v = 1/F_v$. With our formula in eq(3) we obtain

$$R_v = \frac{1}{F_0(\phi - 0.05)^2}. \quad (7)$$

As such we would expect to see divergent behavior at $\phi \approx 0.05$, indeed we do for both crystal structures as illustrated in Figure 3. Both ice types appear to have the same critical threshold for vertical DC conductivity at $\phi \approx 0.05$, which does not allow us to use the critical behavior to determine the ice type. It should be noted that we see a slower rate of divergence at the critical threshold of $\phi \approx 0.05$ in our data from SIPEX II than that compared to SIPEX I. While the reason for this is not clear, the columnar ice during SIPEX I was young, thin (30-60cm) and much less disturbed from its initial formation. In contrast, the columnar ice measured during SIPEX II came from much thicker (1.2-2.5m), relatively older ice, often a part of rafted ice. As a result small deformations in the columnar structure may lead to *average* electrical behavior more like of granular ice as vertical connections between ice crystals would not be as disjoint as in undeformed columnar sea ice.

4.2 Local Variability

As discussed above, we expect to see larger variability in the vertical formation factor F_v on local scales in granular ice than in columnar ice. In fact this is what see when comparing F_v vs ϕ on a core by core basis. Examples of this data are summarized in Fig 4. For samples of columnar ice it is apparent that F_v varies continuously with ϕ with the exception of 1 data point in cores 50 and 51, which incidentally occurs at the cusp of the typical c-curve of salinity vs depth. For the samples of granular ice no clear relationship is immediately apparent. In core 98, for example, there are 5 data points with $\phi \approx 8\%$ which take on different values of F_v between $F_v = 0.01$ and $F_v = 0.024$ more then doubling the conductivity. This is presumed to be a result in differences in vertical connectivity at the same brine volume fractions in granular ice.

In order to quantify the variabilities we assume a power law behavior in accordance with Archie's Law eq 6 and preform linear best fits of the linearized log-log data. In the first set of fits we do not assume $a = 1$ as a way to test for local linear dependence. The results are summarized in table 4.2. When comparing the R^2 statistics for the columnar vs granular samples, we see higher values for columnar ice then for granular ice indicating a higher likelihood of linear correlation. In the columnar samples R^2 ranges from $R^2 = 0.43$ to $R^2 = 0.92$ while the range for the granular samples is $R^2 = 0.014$ to $R^2 = 0.28$ with only 3 of the 7 above $R^2 = 0.05$. Core 54 was a mix of mostly columnar and some large grain granular ice and also shows strong correlation with an R^2 value of 0.74. We would expect columnar ice to be the controlling factor in a mixed sample as it should be the vertical connections which dominate the behavior of F_v .

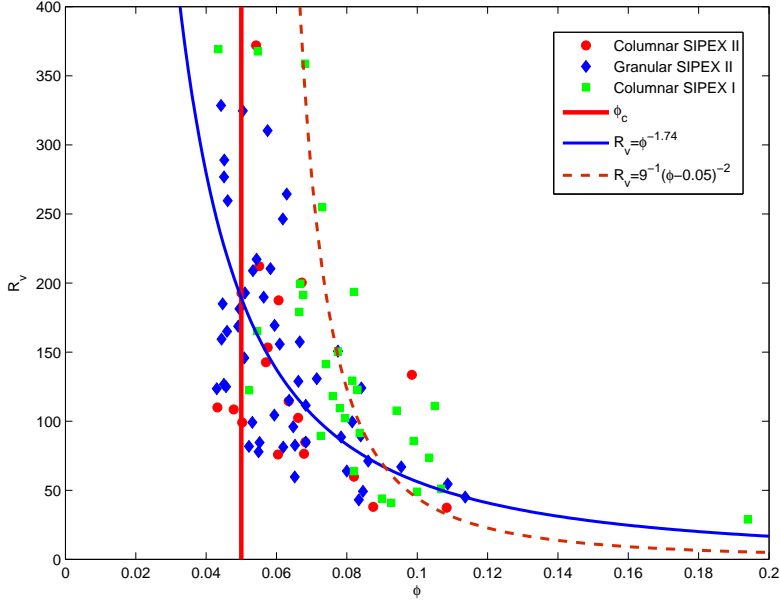


Figure 3: Here we display all of our granular and columnar data in comparison with predictions of the vertical resistivity factor R_v coming from Archie's law with $m = 1.75$ (solid curve) and Percolation Theory(dashed curve). Diamonds represent granular ice , circles columnar ice from SIPEX II and squares columnar ice from SIPEX I in 2007. We note divergent behavior at $\phi \approx 0.05$ where we see departure from Archie's law.

When comparing the P-values for slope of columnar vs granular ice, we see much lower P-values for columnar ice than for granular ice. In this case a low P-value implies a rejection of the null hypothesis of no correlation, while a high P-value implies a lack of linear correlation. Typically, a P-value above $P = 0.5$ is considered grounds to accept the null hypothesis of no correlation. In the columnar samples all of the P-values fall below this threshold with values ranging from $P = 0.008$ to $P = 0.15$ for the slopes while in the granular ice 4 of the 7 cores have P-values above 0.7, with the other 3 ranging from $P = 0.21$ to $P = 0.35$. When comparing the standard errors of the slope for the two data sets, we find that the columnar samples vary less from the model than granular samples with standard errors varying from $S = 0.30$ to $S = 0.88$. The range for granular samples is $S = .87$ to $S = 2.12$. All of these statistics point to a higher variation in the vertical conductivity of granular sea ice in a local region.

Assuming Archie's Law with $m = 1.75$ and $a = 1$ is a good model for the

Core	Ice Type	R^2	Slope	Std. Error	P-value	Intercept	Std. Error	P-Value
44	Col	0.92	1.90	0.3	0.008	0.25	0.37	0.54
50	Col	0.44	1.56	0.88	0.14	-0.21	0.98	0.83
51	Col	0.43	1.38	0.8	0.15	-0.24	0.99	0.82
54	Mix	0.74	2.41	0.58	0.006	0.65	0.72	0.39
69	Gra	0.02	0.43	1.42	0.71	-1.65	1.12	0.28
75	Gra	0.05	-0.36	0.96	0.78	-2.60	1.26	0.18
77	Gra	0.28	2.99	2.12	0.21	1.57	2.60	0.57
79	Gra	0.018	0.55	1.81	0.77	1.40	2.30	0.50
98	Gra	0.014	0.07	0.97	0.95	-1.90	1.19	0.20
99	Gra	0.22	01.20	1.28	0.35	-0.44	1.28	0.70
108	Gra	0.17	0.96	0.87	0.31	-1.02	1.10	0.39

Table 1: Here we present the results of the linear regression analysis where the scaling factor a in Archie’s Law was allowed to be chosen by the data. We see strong linear correlation and less variability in columnar ice than in granular ice.

vertical conductivity we would expect to obtain a linear fit with a slope close to the exponent 1.75 and intercept close to zero. For our columnar ice samples we obtain Archie exponents ranging from $m = 1.56$ to $m = 1.90$ and y intercepts ranging from $b = -0.24$ to $b = 0.25$ corresponding to range of scaling factors of $a = 0.60$ to $a = 1.80$. In the granular ice samples we see drastically different results with exponents ranging from $m = 0.43$ to $m = 2.99$ with 5 of the 7 all less than 1. The y intercepts range from $b = -2.60$ to $b = 1.57$ with 6 of the 7 having magnitude larger than 1. This corresponds to a range of scaling factors of $a = 0.003$ to $a = 37.2$. However as shown in Fig 3 we find that for the data set as a whole, both columnar and granular ice are well represented by the model $F_v = \phi^{1.75}$ for $\phi > 0.05$. It is thus useful to repeat our analysis of the log-log linearized data forcing the scaling factor to be $a = 1$. The results are summarized in table 4.2. When we do this we see excellent agreement with the model for both ice types suggesting that, on average, Archie’s Law is indeed a good model.

5 Topological Data Analysis of Microstructure

In order to further investigate the differences in granular and columnar microstructure variability we provide an analysis of x-Ray Micro-Ct imagery of the porespace of both materials.

A description of the computational methodology Topological data analysis (TDA) is a relatively young field arising from the classic algebraic topology in mathematics. It has been proven successful in several scientific fields. For instance, ???.

Generally speaking, the main idea of TDA is to study the *shape* of data in the form of Betti numbers. *Betti numbers* counts k -th dimensional holes, denoted by β_k . For instance, 0-dimensional hole represents connected components, 1-

Core	Ice Type	R^2	Slope	Std. Error	P-value
44	Col	0.999	1.73	0.02	9×10^{-8}
50	Col	0.995	1.75	0.07	2×10^{-6}
51	Col	0.990	1.57	0.06	1×10^{-6}
54	Col	0.990	1.88	0.02	4×10^{-11}
69	Gra	0.990	1.75	0.06	2×10^{-8}
75	Gra	0.997	1.69	0.05	6×10^{-5}
79	Gra	0.993	1.69	0.06	8×10^{-8}
98	Gra	0.995	1.65	0.06	8×10^{-6}
99	Gra	0.994	1.68	0.05	6×10^{-7}
108	Gra	0.996	1.76	0.06	6×10^{-9}

Table 2: Here we present the results of the linear regression analysis with the scaling factor $a =$ for Archie’s law. In this case we strong correlation in both columnar and granular data.

dimensional hole represents circles, tunnels, 2-dimensional hole can be thought of voids. For example, consider an object depicted in the form of a 2D binary image as shown in Figre 5. One may view binary images in two different ways. One is to view black pixels are present while white pixels are null and vice versa. If we consider the black pixels are present, then the Betti number of Figre 5 is $\beta_0 = 1$ which is the black background, and $\beta_1 = 8$ because there eight regions enclosed by the black pixels. On the other hand, if we consider white pixels are present, the Betti numbers of Figre 5 is $\beta_0 = 8$ because there are eight disconnected white regions, and $\beta_1 = 0$ because there is no black region enclosed by white one. Formal mathematical definition of Betti numbers requires the homology theory (ref). Also, to study the shape, one needs to have a concrete way to represent the object. There are two common ways to achieve it—simplicial complex and cubical complex. Simplicial complex is often used in point cloud data. In this work, we use cubical complexes, where the building blocks are intervals, squares. It is a natural to use cubical complexes to study images because each pixel can be thought as a square.

Some interpretation of what the TDA says about the ice

6 Conclusion

In all, over 81 direct measurements of the DC vertical conductivity of Antarctic sea ice were made and matched to their crystallographic structure. The measurements compare well to a number of established results [13, 30, 21, 20] . While no detectable difference in the vertical conductivity was found between the ice types on average, a higher degree of local variability of the vertical formation factor F_v was found in granular ice. This is most likely related to effect the crystallographic structure has on the way in which vertical connections form in the pore spaces of the two ice types. This implies that measurements of F_v could be used to distinguish between ice types. This is paramount when consid-

ering the remote monitoring of sea ice through out a season. The vertical fluid permeability in particular is sensitive to crystallographic structure and exhibits different critical behavior depending on the ice type. Columnar ice is effectively impermeable for brine volume fractions below $\phi_c \approx 5\%$ [14] while for granular ice there is a critical threshold of closer to $\phi_c \approx 10\%$ [15]. This has severe implications for the biological and physical processes in the ice and thus any models used to understand them. This work demonstrates that that the vertical component of the bulk conductivity could be used to aid in the determination of crystallographic structure of sea ice using electrical methods.

References

- [1] G. E. Archie. The electrical resistivity log as an aid in determining some reservoir characteristics. *Trans. Am. Inst. Min. Metal. Petrol. Eng.*, 146:54–64, 1942.
- [2] U. Bleil and J. Thiede. *Geological History of the Polar Oceans: Arctic vs Antarctic*. Kluwer Academic Publishers, P.O box 17, 3330 AA Dordrecht, The Netherlands, 1990.
- [3] C. Bock and H. Eicken. A magnetic resonance study of temperature-dependent microstructural evolution and self-diffusion of water in Arctic first-year sea ice. *Ann. Glaciol.*, 40:179–184, 2005.
- [4] R. G. Buckley, M. P. Staines, and W. H. Robinson. In situ measurements of the resistivity of Antarctic sea ice. *Cold Reg. Sci. Technol.*, 12(3):285–290, 1986.
- [5] A. Cherkaev. *Variational Methods for Structural Optimization*. New York: Springer-Verlag;, Cambridge, 2000.
- [6] H. Eicken. The role of sea ice in structuring Antarctic ecosystems. *Polar Biol.*, 12:3–13, 1992.
- [7] H. Eicken. Factors determining microstructure, salinity and stable-isotope composition of antarctic sea ice: Deriving modes and rates of ice growth in the weddell sea. *AGU Antarctic Research Series*, 74, 1998.
- [8] H. Eicken. Growth, microstructure and properties of sea ice. In D. N. Thomas and G. S. Dieckmann, editors, *Sea Ice: An Introduction to its Physics, Chemistry, Biology and Geology*, pages 22–81. Blackwell, Oxford, 2003.
- [9] H. Eicken, T. C. Grenfell, D. K. Perovich, J. A. Richter-Menge, and K. Frey. Hydraulic controls of summer Arctic pack ice albedo. *J. Geophys. Res. (Oceans)*, 109(C18):C08007.1–C08007.12, 2004.

- [10] C. H. Fritsen, V. I. Lytle, S. F. Ackley, and C. W. Sullivan. Autumn bloom of Antarctic pack-ice algae. *Science*, 266:782–784, 1994.
- [11] K. Golden. Convexity and exponent inequalities for conduction near percolation. *Phys. Rev. Lett.*, 65(24):2923–2926, 1990.
- [12] K. M. Golden, S. F. Ackley, and V. I. Lytle. The percolation phase transition in sea ice. *Science*, 282:2238–2241, 1998.
- [13] K. M. Golden, H. Eicken, A. Gully, M. Ingham, K. A. Jones, J. Lin, J. E. Reid, C. S. Sampson, and A. P. Worby. Electrical signature of the percolation threshold in sea ice. Submitted.
- [14] K. M. Golden, H. Eicken, A. L. Heaton, J. Miner, D. Pringle, and J. Zhu. Thermal evolution of permeability and microstructure in sea ice. *Geophys. Res. Lett.*, 34:L16501 (6 pages and issue cover), doi:10.1029/2007GL030447, 2007.
- [15] K. M. Golden, A. Gully, C. Sampson, D. Lubbers, and J. L. Tison. Fluid transport in Antarctic sea ice. In preparation, 2011.
- [16] A. Gully, J. Lin, E. Cherkaev, and K.M. Golden. Bounds on the complex permittivity of polycrystalline composites by analytic continuation. *Proceedings of The Royal Society A*, 2014.
- [17] C. Haas, S. Gerland, H. Eicken, and H. Miller. Comparison of sea-ice thickness measurements under summer and winter conditions in the Arctic using a small electromagnetic induction device. *Geophysics*, 62:749–757, 1997.
- [18] C. Haas, M. Nicolaus, S. Willmes, A. Worby, and D. Flinspach. Sea ice and snow thickness and physical properties of an ice floe in the western weddell sea and their changes during spring warming. *Deep Sea Research II*, 55:936–974, 2008.
- [19] M. O. Jeffries, R.A. Shaw, K. Morris, A. L. V., and H.R. Krouse. Crystal structure, stable isotopes ($d_{18}O$), and development of sea ice in the ross, amundsen, and bellingshausen seas, antarctica. *Cold Regions Science and Technology*, 99, 1994.
- [20] K. A. Jones, A. J. Gough, M. Ingham, A.M. Mahoney, P.J. Langhorne, and T. G. Haskell. Detection of differences in sea ice crystal structure using cross-borehole dc resistivity tomography. *Cold Regions Science and Technology*, 78:40–45, 2012.
- [21] K. A. Jones, M. Ingham, D. J. Pringle, and H. Eicken. Temporal variations in sea ice resistivity: resolving anisotropic microstructure through cross-borehole dc resistivity tomography. *J. Geophys. Res.*, 115:C11023, doi:10.1029/2009JC006049, 2010.

- [22] M. P. Lizotte and K. R. Arrigo, editors. *Antarctic Sea Ice: Biological processes, interactions and variability*. American Geophysical Union, Washington D.C., 1998.
- [23] V. I. Lytle and S. F. Ackley. Heat flux through sea ice in the Western Weddell Sea: Convective and conductive transfer processes. *J. Geophys. Res.*, 101(C4):8853–8868, 1996.
- [24] R. Maillet. The fundamental equations of the electrical prospecting. *Geophysics*, 12(4):529–556, 1947.
- [25] T. Maksym and M. O. Jeffries. A one-dimensional percolation model of flooding and snow ice formation on Antarctic sea ice. *J. Geophys. Res.*, 105(C11):26,313–26,331, 2000.
- [26] T. Maksym and T. Markus. Antarctic sea ice thickness and snow-to-ice conversion from atmospheric reanalysis and passive microwave snow depth. *J. Geophys. Res.*, 113:C02S12, doi:10.1029/2006JC004085, 2008.
- [27] G. W. Milton. *Theory of Composites*. Cambridge University Press, Cambridge, 2002.
- [28] R. M. Morey, A. Kovacs, and G.F.N Cox. Electromagnetic properties of sea ice. *Cold Reg. Sci. Technol.*, 9:53–75, 1984.
- [29] A. Omstedt. An investigation of the crystal structure of sea ice in the bothnian bay. Technical Report, Swedish Administration of Shipping and Navigation, 1985.
- [30] J.E. Reid, A. Pfaffling, A.P. Worby, and J.R. Bishop. In situ measurements of the direct-current conductivity of antarctic sea ice: implications for air-borne electromagnetic sounding of sea-ice thickness. *Annals of Glaciology*, 54:217–223, 2006.
- [31] S. Rysgaard, J. Bendtsen, L. T. Pedersen, H. Ramløv, and R. N. Glud. Increased CO₂ uptake due to sea ice growth and decay in the Nordic Seas. *J. Geophys. Res.*, 114:C09011, doi:10.1029/2008JC005088, 2009.
- [32] C. Sampson, K. M. Golden, A. Gully, and A. P. Worby. Surface impedance tomography for Antarctic sea ice. *Deep Sea Res. II*, 58:1149–1157, 2011.
- [33] A. Stogryn and G. J. Desargant. The dielectric properties of brine in sea ice at microwave frequencies. *IEEE Trans. Antennas Propagat.*, AP-33(5):523–532, 1985.
- [34] D. N. Thomas and G. S. Dieckmann, editors. *Sea Ice, Second Edition*. Wiley-Blackwell, Oxford, 2009.
- [35] F. Thyssen, H. Kohnen, M.V. Cowan, and G. W. Timco. Dc resistivity measurements on the sea ice near point inlet, n.w.t. (baffin island). *Polarforschung*, 44:117–126, 1974.

- [36] S. Torquato. *Random Heterogeneous Materials: Microstructure and Macroscopic Properties*. Springer-Verlag, New York, 2002.
- [37] S. Torquato and D. C. Pham. Optimal bounds on the trapping constant and permeability of porous media. *Phys. Rev. Lett.*, 92:255505:1–4, 2004.
- [38] H. J. Trodahl, M. J. McGuiness, P. J. Langhorne, K. Collins, A. E. Pantoja, I. J. Smith, and T. G. Haskell. Heat transport in McMurdo Sound first-year fast ice. *J. Geophys. Res.*, 105(C5):11347–11358, 2000.
- [39] W. F. Weeks and S. F. Ackley. The growth, structure and properties of sea ice. *CRREL Monograph 82-1*, page 130 pp., 1982.
- [40] A. P. Worby and R. A. Massom. The structure and properties of sea ice and snow cover in east antarctic pack ice. *Res. Rep.*, 1995.

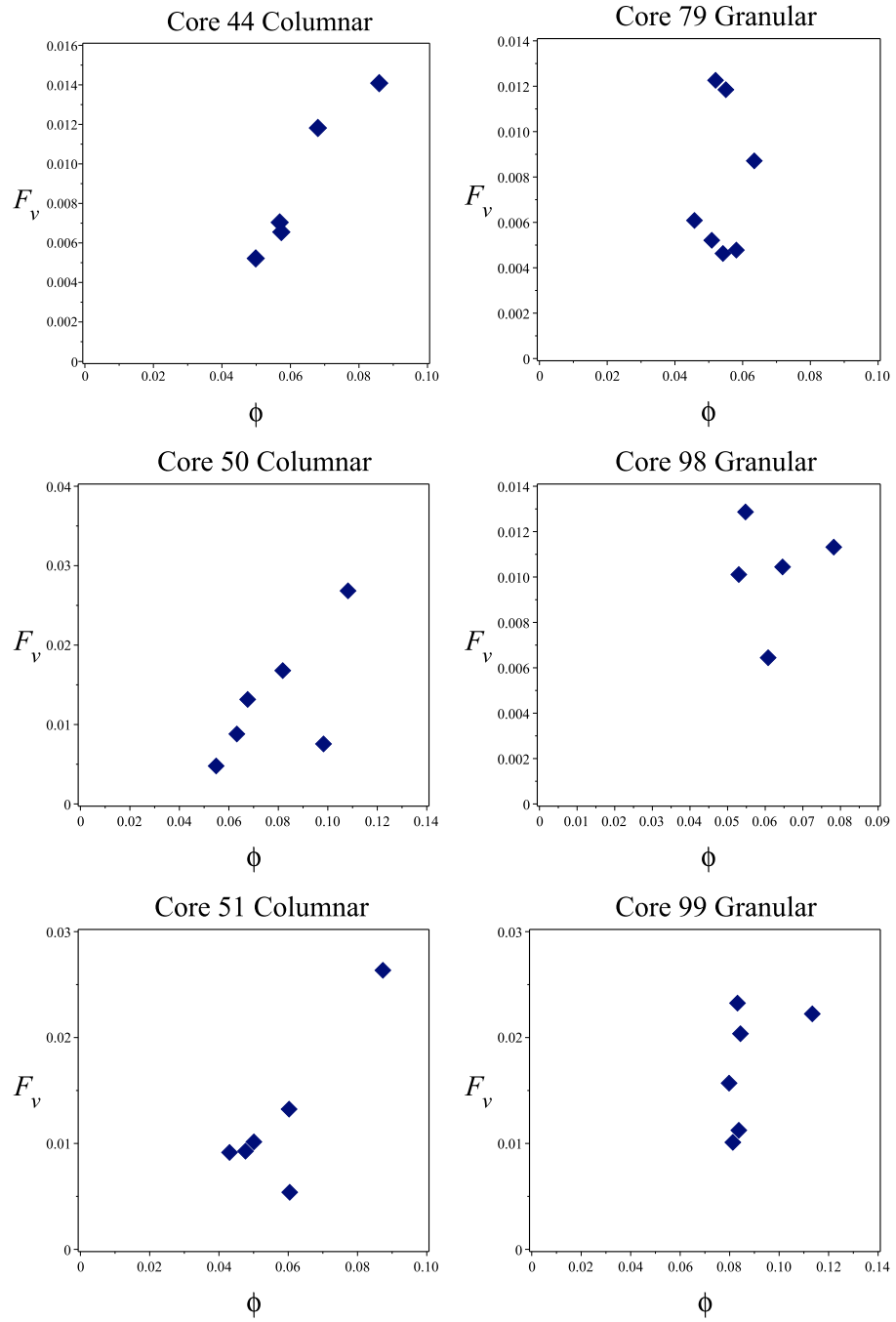


Figure 4: Left Column: Three plots from Cores 44,50,51 of F_v vs ϕ for columnar ice showing continuous behavior. Right Column: Three plots of Cores 77, 79, 99 showing high variability for similar grain volume fractions

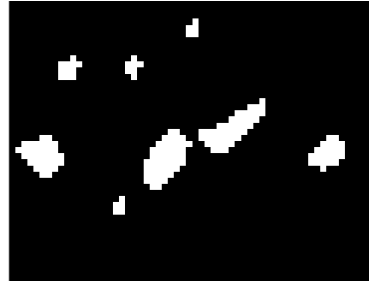


Figure 5: The Betti numbers of a binary image from one of 2D slices of columnar ice. Betti number of black pixels is $\beta_0 = 1$ and $\beta_1 = 8$. On the other hand, Betti number of white pixels is $\beta_0 = 8$ and $\beta_1 = 0$.

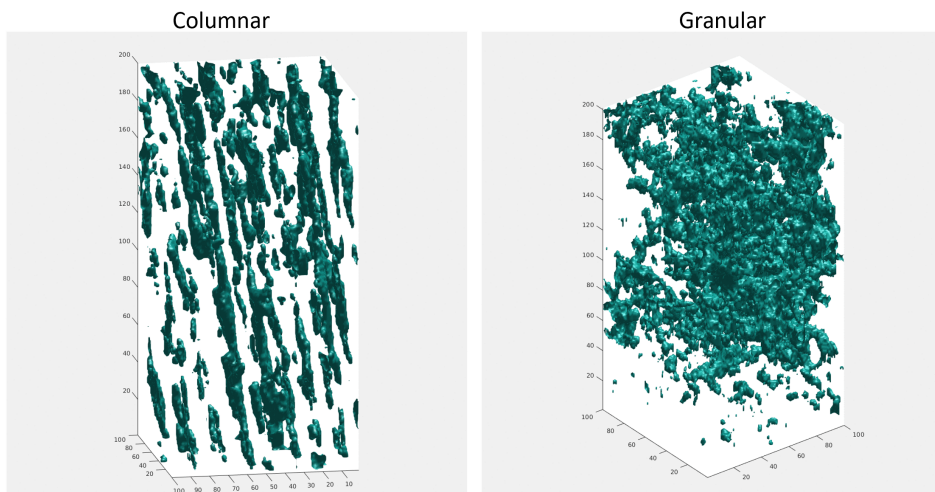


Figure 6: Left: An example of columnar sea ice microstructure whose pore space is constrained to exist between laminate layers of ice crystals. Right: An example of Granular sea ice microstructure whose pore space is much more isotropic.

The Ice is "Empty Space"			
Columnar White	b0	b1	b2
3	9783	5940	86
4	9637	4022	34
5	9992	3115	9
6	9069	1932	2
7	9548	1278	1
8	12767	1841	0
12	11594	1087	0
15	11029	781	0
18	10048	499	0

The Brine is "Empty Space"			
Columnar	b0	b1	b2
3	195	6567	7144
4	65	4465	7185
5	21	3290	7377
6	11	2380	7395
7	5	1606	7701
8	5	1798	9764
12	4	987	9101
15	2	792	8845
18	0	574	8266

Figure 7: The betti-numbers for the columnar microstructure viewing the ice phase as "empty space" (left) and the brine phase as "empty space" (right). Note the rapid increase in complexity near the $T = -5^\circ$ threshold, corresponding to the rule of fives.

The Ice is "Empty Space"				The Brine is "Empty Space"			
Granular White	b0	b1	b2	Granular	b0	b1	b2
3	22087	11504	289	3	1051	12856	13906
4	25138	9031	132	4	599	10260	16156
5	22565	7351	104	5	486	8485	14521
6	22604	7463	113	6	508	8593	14581
7	20089	5840	64	7	328	6797	13044
9	23565	5249	55	9	299	6134	15699
11	23463	3887	44	11	200	4428	16060
13	35724	3058	7	13	91	3688	24507
18	17811	2072	13	18	94	2294	12673

Figure 8: The betti-numbers for the granular microstructure viewing the ice phase as "empty space" (left) and the brine phase as "empty space" (right). Note the rapid increase in complexity above $T = -4^\circ$ threshold, corresponding to the $\phi = 0.1$ threshold for fluid permeability in granular ice. It should also be noted that before this threshold there is much more complexity than that of columnar ice before its threshold of $\phi = 0.05$.